Development and Testing of a 120 kW RF Power Processing Unit for the VASIMR® System

Matthew Giambusso,[1] Jared P. Squire,[2] Franklin R. Chang Díaz,[3] and Aidan M. H. Corrigan[4]
Ad Astra Rocket Company, Webster, Texas, 77598, USA

Tim Hardy[5]
Aethera Technologies Limited, Halifax, Nova Scotia, B3S 1B5, Canada

In January of 2020, Ad Astra Rocket Company began operating a technology readiness level (TRL) 5 power processing unit (PPU) developed for the ion cyclotron heating (ICH) stage of the VASIMR® VX-200SS™ plasma thruster prototype. Aethera Technologies, of Halifax NS, Canada, developed this PPU under contract with Ad Astra and with additional support from the Canadian Space Agency. The PPU uses modern, GaN power electronics that have the potential for spaceflight. Weighing only 52.9 kg, including a 15 kg magnetic shield, the unit produces up to 120 kW of RF power at frequencies of 0.4 to 1.0 MHz, with a DC-to-RF power conversion efficiency of 98%. During a 4-hour test with a water-cooled resistive load, Ad Astra operated the PPU in thermal steady state at full power while under high vacuum. The VX-200SS™ magnet was fully energized during the last hour of the test, but the field had no significant effect on the unit in its installed location (2 m from the thruster axis). The new PPU is now a permanent part of the upgraded VX-200SS™ system, replacing a TRL-4 unit that resides outside of the test chamber. Ad Astra has since resonated the ICH stage while operating at a total (helicon plus ICH) power of 100 kW, easily tuning the new unit to the plasma circuit. Additionally, Aethera has developed a commercial PPU, of similar design and performance, but operating at the higher frequency (~7 MHz) required by the helicon stage of a VASIMR® system. Minor changes will adapt the commercial PPU to the VX-200SS™. The complete (helicon and ICH) radio frequency power subsystem will then operate in a relevant vacuum, thermal, and magnetic environment.

I. Introduction

The Variable Specific Impulse Magnetoplasma Rocket (VASIMR®) system is a two-stage, radio frequency (RF) powered, fully magnetized plasma thruster designed for in-space propulsion. The rocket uses a helicon type plasma source to ionize a propellent, and ion cyclotron heating (ICH) to accelerate the ions of the resulting plasma. A superconducting magnet surrounds the rocket core, providing the magnetic field necessary for the two stages to function (see Fig. 1). The magnetic field also insulates the rocket core from the plasma and acts as a nozzle which guides the expansion of the rocket's exhaust. An overview of the technology can be found in Ref. [1].

[1] Senior Research Scientist.
[2] Senior Vice President of Research, AIAA Associate Fellow.
[3] Chief Executive Officer, AIAA Senior Member.
[4] Senior Mechanical Engineer, AIAA Member.
[5] Chief Technology Officer.

VASIMR® systems have recently been designed to use argon gas as a propellant, although many other gases are possible. Using argon, a single VASIMR® thruster can achieve a specific impulse of 4900 seconds while operating at a power level of 200 kW [2].

The VX-200SS™ is a 100 kW, thermal steady-state variant of the earlier 200 kW VX-200™ pulsed prototype, developed privately by Ad Astra Rocket Company. Its primary goals are to advance the VASIMR® technology to TRL 5 and to demonstrate the thermal management necessary for continuous, long-duration operation at 100 kW of DC input power. The VX-200SS™ program was initiated in 2015 as a public-private partnership between NASA and Ad Astra under the Next Space Technologies for Exploration Partnership Program (NextSTEP).

In addition to the thermal management objectives for the VX-200SS™ prototype, the NextSTEP program also required the thermal steady-state demonstration of the rocket's Power Processing Units (PPUs) in the vacuum environment. This objective was not funded by NASA but enabled by a separate and parallel program with Aethera Technologies of Halifax, NS, Canada and jointly funded by Ad Astra and the Canadian Space Agency (CSA). This paper describes the TRL-5 PPU development and testing process.

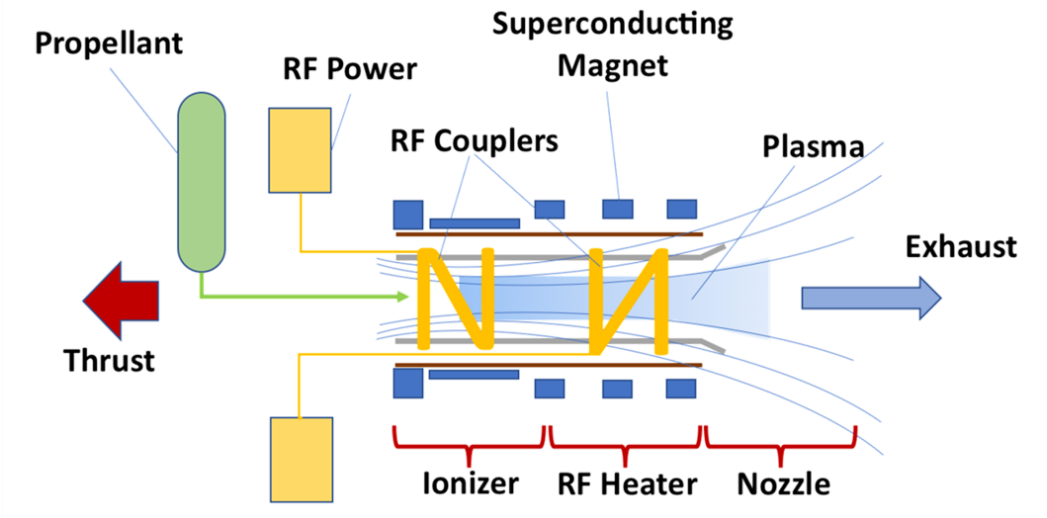

Fig. 1 Simplified schematic of a VASIMR® system.

A. Power Processing Units in a VASIMR® System

PPUs are a critical element of any electric propulsion (EP) system; they provide power from the solar array to the thruster. The thruster in turn uses the power to produce and accelerate plasma. Plasmas are inherently challenging as electrical loads, particularly at high power. PPUs ideally have a high efficiency (DC to coupled power in the plasma), light weight, and tolerance to variations in the plasma load.

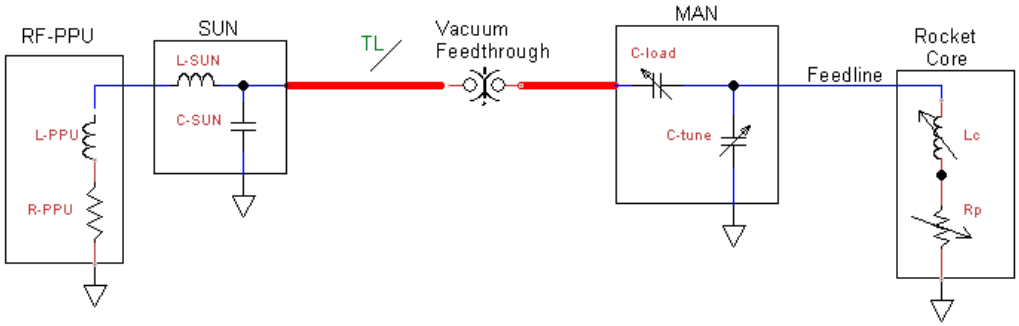

Fig. 2 Simplified electrical schematic of a VASIMR® RF circuit, showing a legacy RF PPU and step-up network (SUN) outside of the vacuum chamber. The SUN transforms the PPU output to match a standard 50Ω transmission line. The matching network (MAN) transforms the impedance back down to match the coupler-plasma circuit.

VASIMR® PPUs have distinctions from those of traditional, electrostatic EP devices [3,4]. First, a VASIMR® thruster uses RF power to drive its helicon and ICH stages. The power coupling scheme takes advantage of natural oscillations in magnetized plasmas (helicon and ion cyclotron waves). These waves propagate without density cutoff and at relatively low frequencies (~1 – 10 MHz), allowing the use of efficient, solid-state power conversion techniques that have advanced with the electrification of society. A second distinction is that VASIMR® requires no neutralization; the plasma is net neutral throughout. The propellant flow, 1st stage power, and 2nd stage power can all be adjusted independently to the meet the requirements of a given operational profile.

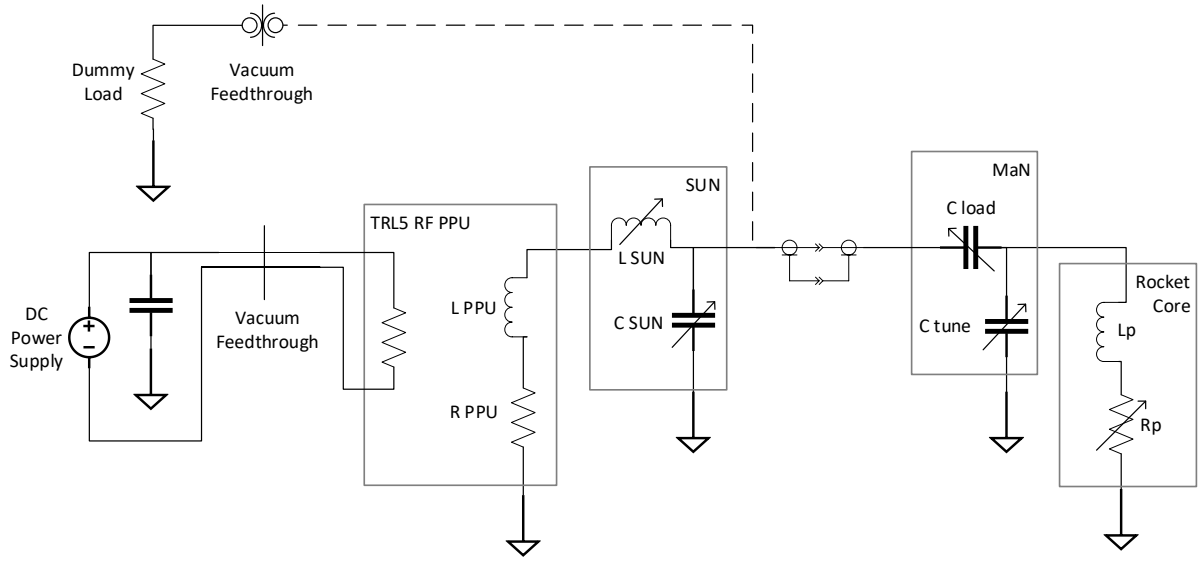

Fig. 3 Updated electrical schematic, showing the VX-200SS™ TRL-5 ICH PPU inside the vacuum chamber with the optional connection to a resistive load for testing.

For efficient RF power coupling from the PPU to the plasma, impedance matching is crucial. As shown in Fig. 3, VASIMR® systems use an adjustable matching network located just outside the rocket core to minimize reflected power to the PPU. This arrangement lends itself to the use of high impedance, low loss, RF transmission lines and remotely located PPUs in spaceflight. RF transmission would be particularly advantageous for high-power (>50 kW) systems which require correspondingly high DC currents (>400 A) from the solar array.

B. Aethera Technologies

For the past 10 years, Ad Astra Rocket Company has used solid-state, TRL-4 PPUs for plasma testing at total (helicon plus ICH) powers up to 200 kW. Aethera Technologies has now developed a TRL-5 PPU for the ICH stage of the VX-200SS™ prototype. The new PPU uses modern, GaN-based power electronics that have the potential for spaceflight. Figure 4 shows a model of the PPU and the completed unit being weighed. With a mass of only 52.9 kg, including a 15 kg magnetic shield, the PPU produces up to 120 kW of RF power at frequencies of 0.4 to 1.0 MHz. The unit is designed for steady-state operation entirely within vacuum. The cylindrical shape minimizes the material required to shield the PPU from the stray field to the VX-200SS™ superconducting magnet. Spaceflight versions may not need as much shielding if they are located near the DC power source. Additionally, spaceflight VASIMR® systems will necessarily be arranged as quadrupole magnets, further reducing the stray field and the necessary shielding for a given location. Without shielding, the existing RF-PPU design would weigh approximately 40 kg.

The technologies used in the design of the ICH PPU also have direct application to the first stage helicon PPU. In fact, Aethera Technologies has already developed a 50 kW, 7 MHz commercial power generator for terrestrial applications. This generator is almost entirely conduction cooled and already has many of the features of the ICH PPU, with an efficiency better than 95%. Application to a TRL-5 helicon PPU will be straightforward.

The remainder of this paper details the design and testing of the TRL-5 ICH PPU.

II. PPU Design

The PPU described here is a solid-state RF power supply that drives the ICH stage of the VX-200SS™ prototype. The PPU is designed to achieve TRL-5 and to incorporate TRL-6 elements where feasible. Table 1 lists the basic specifications. The major sections of the PPU system are listed in Table 2.

Table 1 RF PPU Specifications

Power	120 kW
Input	270 to 350 VDC
Output Frequency	0.4 to 1.0 MHz
Efficiency (RF_{out}/DC_{in})	98%
Size (LxHxW)	972 mm x 255 mm x 255 mm
Mass (with magnetic shield)	52.9 kg

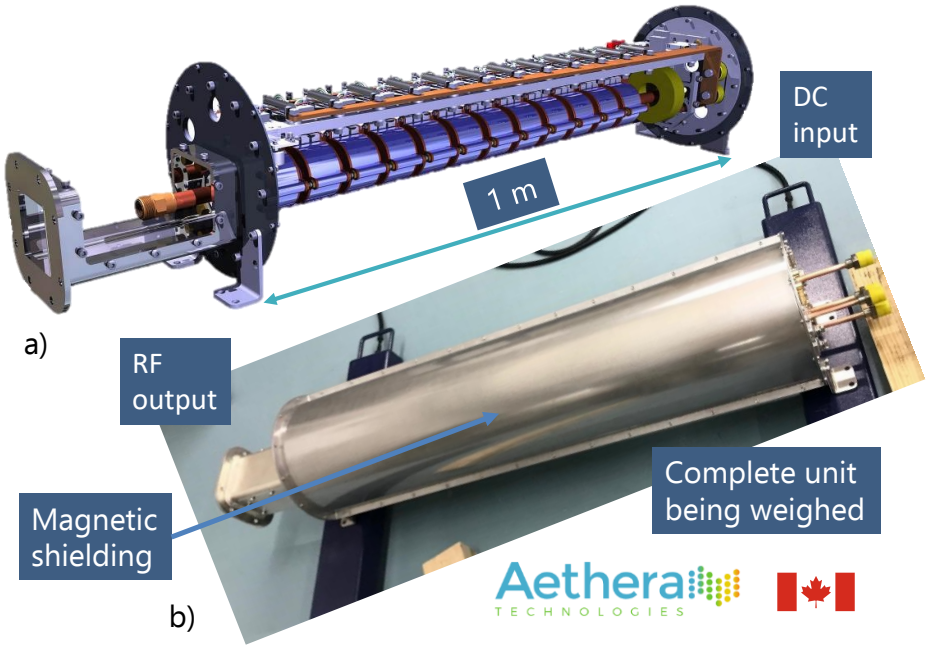

Fig. 4 a) CAD model of the TRL-5 PPU. b) The completed PPU with shielded enclosure.

Table 2 PPU Subsystems

Power Amplifiers
RF Power Combiner
Master Controller
Current, Voltage and Flow Sensors
DC Distribution, Protection, and EMC Filter
Cooling System
Supporting Structure
Enclosure

A. Power Component Design

1. Power Amplifiers

There are 12 power amplifier (PA) boards, each designed to contribute 10 kW of RF output at full power. The PA circuits are classified as Voltage Mode Class D (VMCD) type, high-efficiency switch mode amplifiers and are configured in an H-bridge topology. The transistors selected offer very high-speed switching, low stored energy, very low on resistance, and a small chip scale package.

The modern HEMTs in the PA circuit enable significant advantages compared to silicon-based, metal–oxide–semiconductor field-effect transistors (MOSFETs):

- increased energy conversion efficiency
- expanded transistor Safe Operating Area (SOA), reducing risk of failure to reach desired power
- reduced overall PPU volume and mass due to the smaller PA size
- reduced magnetic shielding required in proximity to the VX-200SS™ dipole
- reduced cooling system volume and mass
- common transistor technology for both the helicon and ICH frequencies, reducing development time and risk for the helicon PPU
- increased radiation tolerance and potential for spaceflight [5-8]

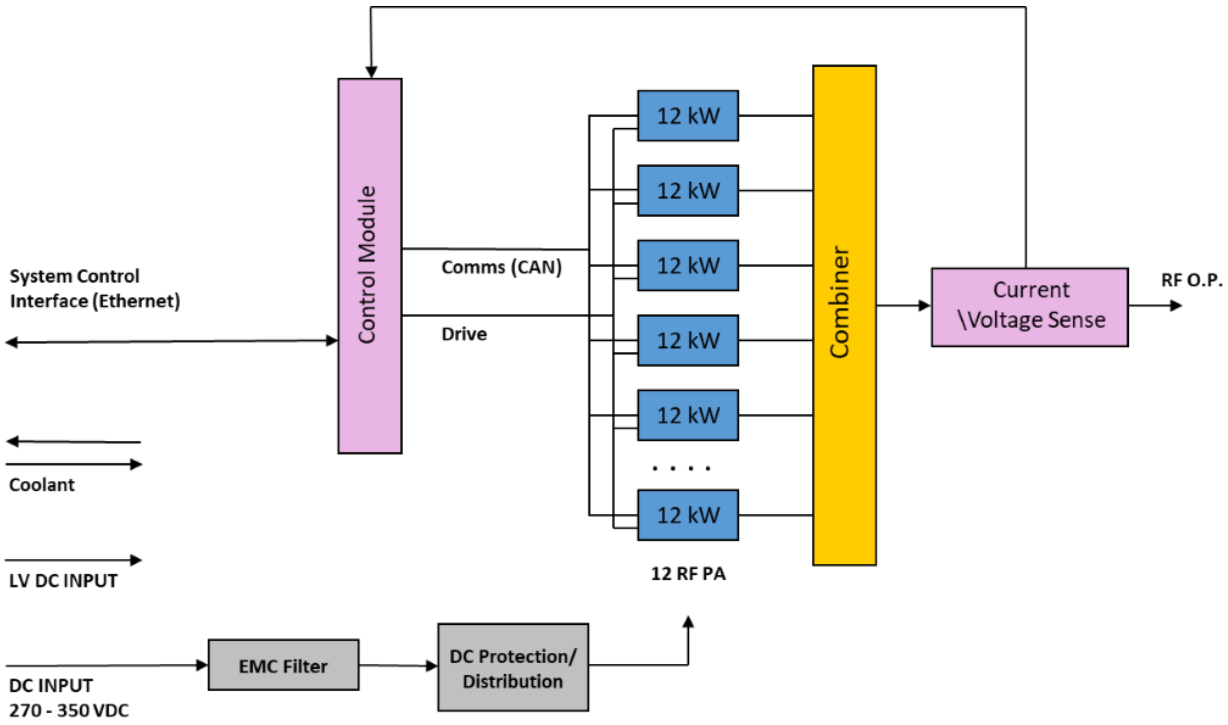

Fig. 5 Functional block diagram of the TRL-5 PPU.

2. Power Combiner

The RF combiner uses a broadband transformer design to sum the power output from the 12 PA boards. Each PA feeds a primary transformer winding. The transformer consists of a series of toroids with ferrite cores. The combiner design is based on a well-established method and was used in the TRL-4 PPUs.

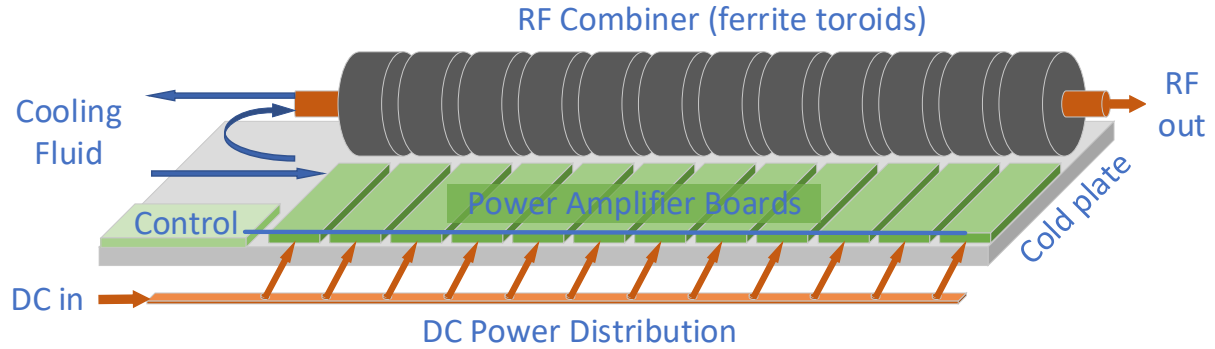

Fig. 6 Simplified diagram of the PPU internals.

3. VSWR tolerance

The Voltage standing wave ratio (VSWR) at the PPU output is an indication of how well the load impedance is matched to the RF generator. A VSWR of 1 is ideal, while higher numbers indicate more reflected power. The power components of the TRL-5 PPU have been designed to allow operation into non-ideal loads, which simplifies the start-up of the VX-200SS™ and makes it easier to adjust power dynamically. Once a desired power is achieved, the VX-200SS™ matching network can typically be used to tune the overall circuit impedance to a VSWR less than 1.1.

Aethera has engineered the PPU with a generous power-VSWR operational envelope, ensuring that the power amplifiers remain within the SOA throughout the operational frequency band. The implementation of VSWR protections is described in section II.B.3., below. The VSWR tolerant design also simplifies the process of vacuum-resonating the ICH stage of the VX-200SS™, which is described later in section III.F.2.

Table 3 PPU Operational VSWR Envelope

Power (kW)	Maximum VSWR
0	3
5	3
20	1.5
100	1.5
120	1.35

4. Efficiency Prediction

The primary losses in the PPU are in the PAs and power combiner, but losses in the DC bus and auxiliary systems were also included in a predictive efficiency analysis. The analysis was performed for a nominal operating frequency with a total output RF power of 100 kW and input voltage of 310 VDC. For the PA, the losses were dominated by the transistor conduction and switching loss. The analysis is summarized in Table 4. The model required 101,704 W DC input power to produce 100,000 W RF output power. The predicted net conversion efficiency of DC to RF power was therefore 98.3%. This analysis is consistent with the component and system measurements described in subsequent sections.

Table 4 Predicted PPU Component Losses at 100 kW RF Output Power

Component	**Loss (W)**
Power Amplifiers	1082
Combiner	513
DC Bus	41
Auxiliary	68
Total	**1704**

B. Control and Protections

An embedded system controls, monitors, and protects the RF PPU from faults. The control system is divided into two main areas: the amplifier control system, which monitors and protects the individual amplifiers with a distributed network; and the master controller, which is responsible for commanding, controlling and monitoring all other aspects of the system. See Fig. 5 for a simplified block diagram of the PPU's functional arrangement.

1. Integrated Control at the Power Amplifiers

Power control is managed at the master control level based on external inputs from the VX-200SS™ control system. The amplifiers are subordinated to the master controller which makes decisions on how many amplifiers should be active at any time to control the PPU output voltage.

Amplifier state commands are passed directly from the master controller to each individual amplifier on the amplifier drive inputs. The amplifier drive inputs are connected to a Field Programmable Gate Array (FPGA) which drives the power transistors.

A microcontroller monitors the status of the amplifier, including key signals related to the power electronics. The microcontroller has bidirectional signaling with the FPGA; it can pass a local inhibit command to the FPGA drive logic. Improper drive logic states or fault conditions monitored by the FPGA may also be signaled back to the microcontroller and the master controller over the serial bus. A functional block diagram of the PA control is shown in Fig. 7.

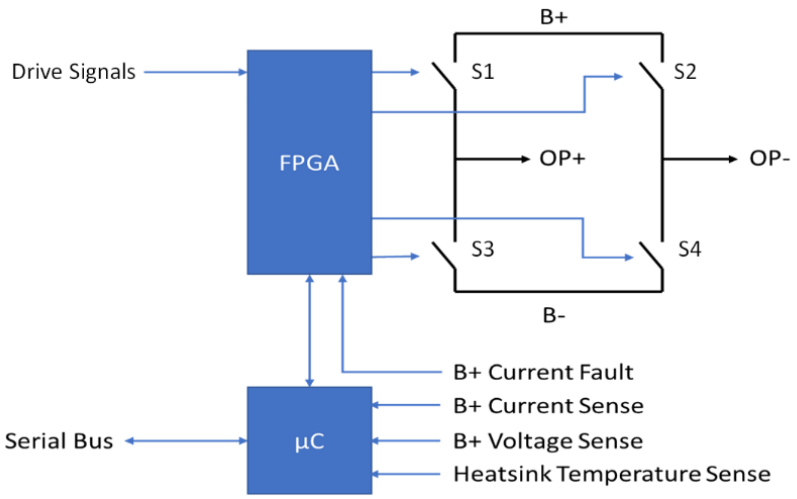

Fig. 7 Control system at each of the 12 amplifier boards. B+ is the DC bus voltage. S1-S4 are the transistor legs comprising the H-bridge amplifier circuit.

The amplifier software is written in C. There is no operating system on the microcontroller, only a basic event loop. The main task of the microcontroller is to monitor the instrumentation on the amplifier and provide that data to the master controller. It can be reprogrammed in system, either with a dedicated programmer or from the master controller, and it has its own on-board flash.

The FPGA is responsible for monitoring and implementing the RF drive signals, along with acting on any fast fault detection. It has internal flash that can be reprogrammed in-system with a dedicated programmer.

Table 5 Amplifier Faults that trigger a local power inhibit

High DC Voltage	B+ voltage exceeding a programmable threshold
High DC Current	DC current exceeding a fixed threshold
High Temperature	Heatsink temperature exceeding a programmable threshold
Drive Signal	Incoming drive signals outside of their normal state

2. Master Control

The master controller is based on a Digital Signal Processor (DSP) and FPGA chipset with sufficient processing power to control the system and generate the PA drive signals. The controller communicates with the outside world over ethernet. The drive signals for the system are generated using the FPGA and a digital-to-analog converter, allowing precise frequencies to be generated.

The master controller is the most complex device in the PPU control system, with most of the software running on the DSP. It is responsible for power control, signal processing, protection, communications, and general supervisory duties in the system. The code is a mixture of C/C++ and assembly. Generally, the code is written in C++ to allow for better testing and code reuse except for performance reasons (requiring assembly) or to allow existing library use (requiring C).

The master controller monitors the RF output voltage using a capacitive attenuator near the output interface. RF output current is sensed using a commercial current transformer (CT) at the low voltage end of the combiner secondary conductor. The controller uses the voltage and current signals to calculate the output power and the load impedance.

In the typical mode of operation, a proportional-integral feedback loop compares the output power to the commanded power from the VX-200SS™ control system. The master controller adjusts the output power by pulse width modulating the active status of the individual PAs. This is done at a frequency (~ kHz) high enough to allow the output power to be controlled smoothly.

3. System Level Protection

The master controller is responsible for protection at the system level. Protective actions are based on information gathered from the system level sensors, the status of the PA's, and the external inhibits. Efficient operation of the PAs depends on fundamental and harmonic load impedances which produce the correct current waveform for low loss operation. Losses increase rapidly when the impedance deviates (VSWR > 1) to produce capacitive currents. The system protections are designed to prevent operation outside of the transistor SOA.

Table 6 System Level Protections

Fast VSWR Protection	Protects against fast load transients that might indicate arcing in the load network. This fast protection reacts quickly in the event of a sudden excursion from the SOA, inhibiting all amplifiers directly via the modulation control lines without intervention from the DSP.
Software VSWR Protection	Prevents exiting the SOA during a controlled power ramp. The DSP software reduces power until the SOA has been re-entered. This situation might be corrected by re-tuning the matching network (see Fig. 3).
Forward Power Limit	Reduces power if the total forward power exceeds 125 kW. Prevents overstressing system level components including the combiner secondary and the DC power bus.

4. External Communication and Command

All communications with the RF-PPU are handled by a 10/100BASE-T Ethernet connection. One TCP/IP port provides a text-based console and a second TCP/IP port provides a binary machine interface (Modbus). Optionally, the unit can stream samples in real time over UDP to a configurable port on an external computer.

During typical operation, the VX-200SS™ operator programs and executes a PPU power ramp via the Modbus interface. This is normally done as part of a command to the larger VX-200SS™ system, although the PPU can be operated independently for testing. The power ramp is a sequence of operating points; each point consisting of the desired output power, the desired frequency, and the elapsed time to reach this combination from the previous point. The text-based console of the PPU is used mostly for troubleshooting and software updates.

The only input to the PPU not over Ethernet is an external hardware inhibit line. This is a low-voltage signal which is used by the VX-200SS™ control system to interlock the PPU output with various system conditions. For example, when operating into the dummy load (see Figures 3 and 14), the VX-200SS™ control system interlocks PPU power with adequate water flow through the load.

C. Mechanical and Thermal Design

1. Mechanical Design

The ICH RF PPU assembly mechanical system was designed to produce a densely packed arrangement of electrical and magnetic components girdling an RF combiner. This design philosophy was adopted to minimize thermal loads, optimize magnetic shielding, and minimize the structural mass of the device. The functional RF PPU assembly is contained within a thin-walled, tubular magnetic shield. Physical interfaces include mounting points, an ethernet connector, a D-sub connector for control power and external inhibit, coolant connections, DC power inputs and an RF power output. The assembly has no moving parts.

The overall dimensions of the ICH RF PPU are listed in Table 1, excluding the interface connections. The width of the PA board is the functional element that drives the length of the assembly. The overall length is consistent with the predicted scale size of a 150 kW VASIMR® engine.

The total dry mass of the assembly is 52.9 kg, with the magnetic shield comprising approximately 15 kg of that total. The specific mass of the PPU is therefore 0.44 kg/kW, which compares favorably to a previously published study of VASIMR® system mass scaling [9].

2. Thermal Design

The functional components are thermally bonded to a central, fluid-cooled heat sink (cold plate). The cold plate forms the main cooling circuit and dissipates heat from the PA boards and combiner cores. Most of the total heat loss in the system is managed by the cold plate, the major exception being that of the secondary RF output winding. The system can run safely at full power with the inlet water temperature as high as 45 °C.

The cooling design was simulated using finite element analysis software. The power transistors are the primary heat source in the PA board assembly. The primary heat source in the combiner is from hysteresis loss in the ferrite cores of the RF transformer.

The output center conductor, the secondary of the RF transformers, is cooled by a ground reentrant tube in tube design. The cooling water is recirculated inside of the RF current carrier tube with a smaller tube inside. The tube-in-tube circuit continues through the PPU's RF output connection to a water-cooled inductor in the ICH step-up network.

D. Electromagnetic Compatibility (EMC) Design

1. Conducted DC Emissions

The RF amplifier decoupling capacitors are a low impedance source of harmonic frequencies which the DC bus will directly conduct to the outside if not filtered. 2.2 µH inductors and high-power capacitive feedthroughs are used to control this emission.

2. Magnetic Shielding

The PPU enclosure is designed to shield the power components from the static field of the VX-200SS™ magnet. The background field was conservatively assumed to be 60 G prior to the mounting location being finalized. The shielding material reduces the internal field strength to a magnitude that is acceptable to the design of the amplifiers and the RF combiner. The PPU enclosure also functions to block radiated emissions *from* the PPU.

The shielding material constitutes a significant portion of the overall mass (~28%). The necessary shielding mass could be reduced in a spaceflight VASIMR® system because the magnets will be arranged as a quadrupole, canceling the overall dipole field and reducing the field strength for a given proximity to the rocket core.

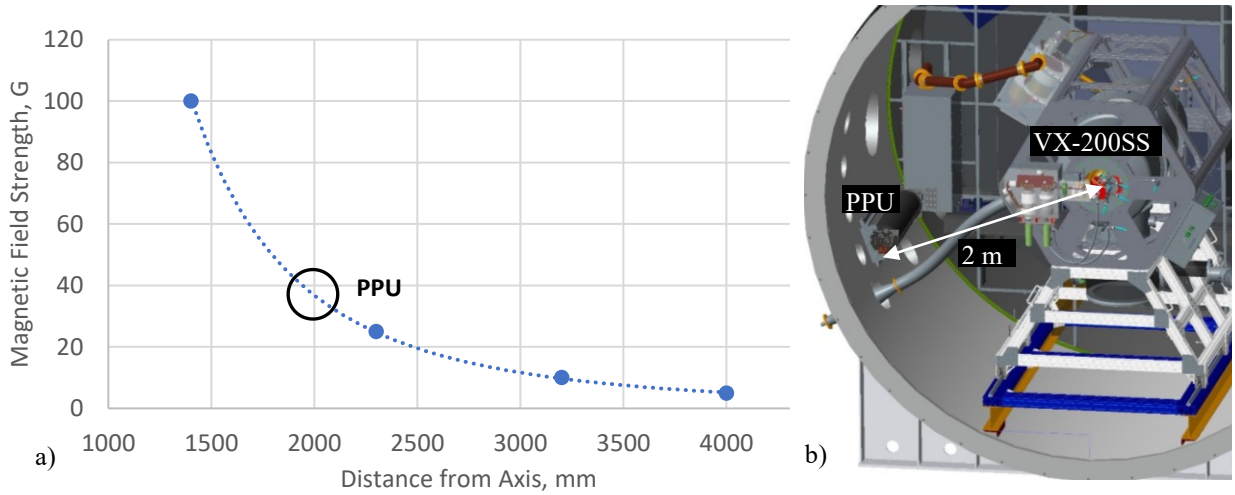

Fig. 8 a) Stray magnetic field strength as a function of radial distance from the midpoint of the VX-200SS™ rocket core axis and b) model of the RF PPU's proximity to the VX-200SS™ magnet.

E. Vacuum Compatibility Design

The PPU is designed to avoid an internal Paschen breakdown and to minimize the gas load to the VX-200SS™ vacuum environment. The unit was required to meet these criteria while at full power in ambient pressures ranging from 10^{-7} to 10^{-4} Torr. Venting holes in the endplates of the enclosure were conservatively sized based on estimates of the internal surface area and material outgassing rates. Low-outgassing materials were used in the PPU subsystems wherever possible. The conductance of the PPU venting area was subsequently considered while developing the initial vacuum test plan (see section III.D.3).

III. PPU Testing

A. Component Testing at Aethera

Prior to the complete unit assembly, Aethera built and tested one power conversion section at full power (greater than 10 kW). Two configurations were tested, one on a bench for DC-to-RF performance assessment and one in a small vacuum chamber for thermal performance validation. Extreme impedance matching conditions were explored to verify robustness. The power element section included a PA, RF combiner toroid set, and a cold plate section. The complete RF PPU comprises 12 of these sections repeated. The single section tested the RF power conversion, integrated PA control, voltage handling and thermal design.

1. Component Benchtop Testing

Performance measurements were carried out on a benchtop in air. Convective cooling effects were minimal. Two measurements were carried out. The first method measured output RF power with an Ion Physics model CM-1-L

current transformer measuring current into a 50 Ω dummy load and a Rohde & Schwarz NRP18T power termination. The second method measured the power loss directly with water calorimetry. Both methods used the input DC power measurement; this came from voltage and current sensors indicated by a Magna Power model TSD500-60 power supply. The RF test frequency was 1 MHz, which was expected to produce slightly higher losses than those predicted by the analysis in Table 4.

For the RF output measurement, the system was tuned such that the measured output power was 10 kW, simulating the entire PPU operating at 120 kW and a nominal input of 300 VDC. The input voltage and current were 299.2 V and 33.9 A, respectively, giving an input DC power of 10.143 kW. The resulting efficiency was P_{out}/P_{in} = 98.6%.

For the calorimetered loss measurement, the output RF power was again tuned to indicate 10 kW. The water flow was adjusted to 1 gpm as measured by an Omega series FL46300 sensor. The cold plate water temperature differential temperature of 0.45 °C ($T_{out} - T_{in}$) was measured by thermocouples and a Fluke 54 II B data logging thermometer with dual input. The differential measurement is more precise than the absolute temperature indication, and baseline measurement with the power elements turned off indicated zero. The heat loss measured in the water was 118 W. Air convective heat loss from the combiner assembly was estimated as less than 10 W, by measuring the surface temperature with an IR camera. The total loss was estimated to be 128 W. The resulting efficiency was $(P_{in} - P_{loss})/P_{in}$ = 98.7%.

2. Component Vacuum Testing

The component vacuum test was intended to measure the temperature rise of the combiner transformer with maximum thermal load (approximately 50 W dissipated); this was the greatest risk in the thermal design. Since all conduction cooling is through the surface at the cold plate, the hottest point on the assembly is at the opposite side of the transformer, which has the longest thermal path. The windings on top of this point are the hottest surfaces on the transformer.

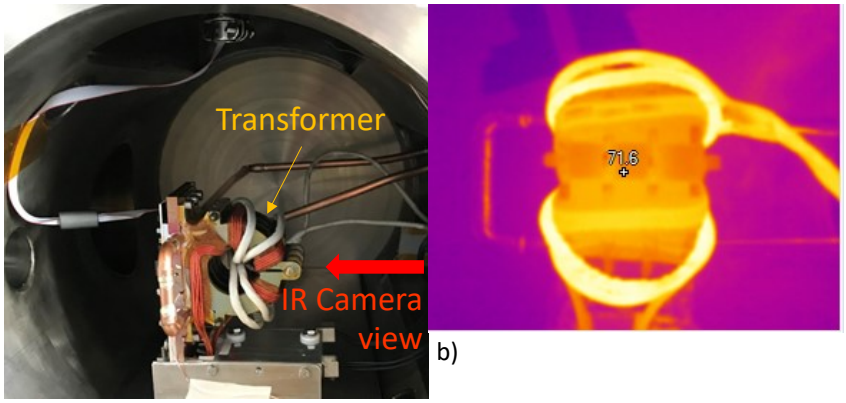

Fig. 9 a) RF combiner transformer and amplifier board configuration inside the vacuum chamber and b) infrared image of the RF combiner at steady state 12 kW operation. The combiner winding temperature was approximately 90 °C, which is within its operating range.

Transformer loss is driven primarily by the input voltage which increases hysteresis loss. Maximum thermal stress occurs at the high end of the input DC voltage range. The vacuum test was therefore carried out at 350 VDC input and output power up to 12 kW, exceeding the total output power requirement. Electrical power measurements were like those described in the benchtop component test. The temperature of the combiner element was captured using a Fluke Model TiS45 infrared camera viewing through a zinc selenide window. Figure 9 shows a thermal image at 12 kW in steady state. Surface temperatures were also measured using Omega ML4C temperature stickers. Vacuum pressure during the test was measured with a Granville-Phillips 356 Micro-Ion Plus Module as approximately 10^{-4} Torr.

Table 7 Component Vacuum Test Results

Maximum Transformer (winding) temperature	90 °C
Cooling Water Temperature	35 °C
Cold Plate Temperature (under transistors)	42 °C
RF Power to Load	12.095 kW
DC Input Power	(350.1 VDC)(34.96 ADC) = 12.24 kW
Measured Efficiency	98.8%

B. Unit Test at Aethera

Before shipment of the completed RF PPU, a representative from Ad Astra traveled to Aethera to participate in a Factory Acceptance Test (FAT) and visually inspect the unit. Aethera only has the facilities to test the PPU in air and up to 20 kW of power. To simulate the equivalent stress of full power on the components, reduced powers were processed into extreme impedance mismatches. The test setup is shown in Fig. 10.

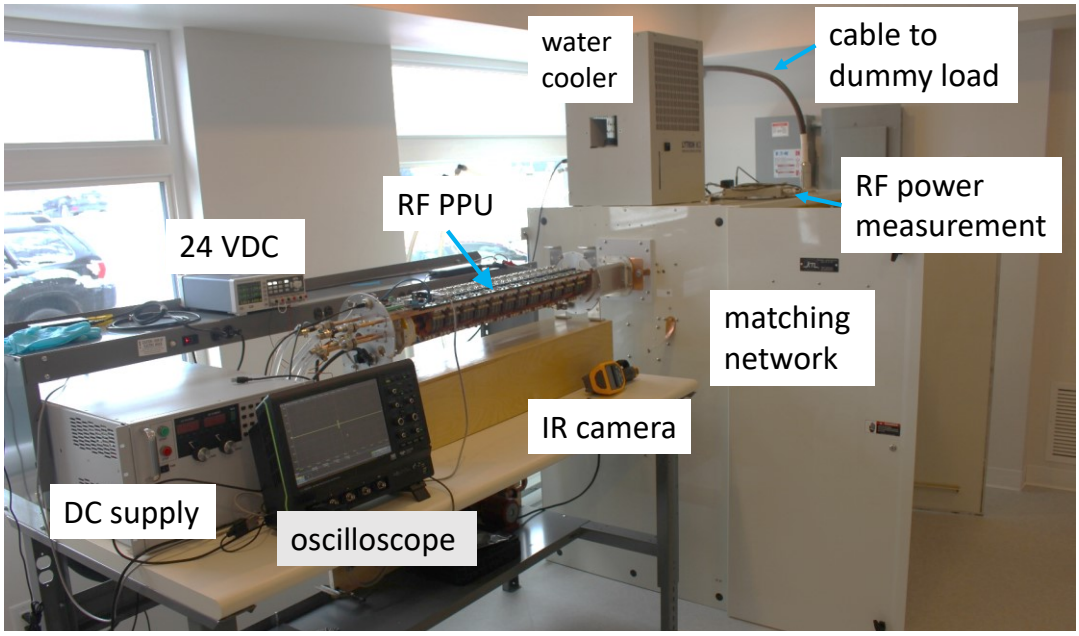

Fig. 10 Bench test of the assembled PPU at partial power (20 kW).

Maximum stress on the power combiner transformers was accomplished at the low end of the design frequency range, 400 kHz, with a load impedance 10 times the optimal value. The transformer temperatures were observed to all stay well within design specification.

High stress on the power transistors was accomplished by processing power at 20 kW and 3 kW into highly capacitive loads with a VSWR of 1.5 and 3, respectively. All parameters were well within component specification.

Hard shut-back fault protection was demonstrated by suddenly applying a dead short to the PPU output while at 20 kW. The unit shut down rapidly and safely without harm multiple times. Testing was also performed at the normal VX-200SS™ operating frequency, the maximum frequency of 1 MHz, and across the voltage range of 270 to 350 VDC.

C. Full Power Bench Test at Ad Astra

After shipment from Aethera, Ad Astra bench-tested the RF PPU to its full 120kW power rating for the first time. Full power was tested at input voltages of 270, 300, and 350 VDC. The newly constructed step-up network inductance and capacitance (see Fig. 3) were adjusted to present a near ideal impedance for these tests (VSWR 1.03). Power was terminated into a 50 Ω, 125 kW, water-cooled, Altronic Research model 97125 dummy load, as shown in Fig. 11. For safety, the PPU's external inhibit lines were interlocked with a flow switch and a temperature switch at the water outlet of the dummy load. In order to supply sufficient water flow (>15 GPM) and cooling to the dummy load for steady state operation, Ad Astra re-configured two previously distinct water systems to be in series: one supplying the requisite head pressure and the other providing the heat rejection capacity (see Fig. 13).

1. Bench Test Measurements

The PPU enclosure was left off for this test, and a Jenoptik IR-TCM640 infrared (IR) camera was trained on the PPU components to check for uniformity or degradation. A Fluke 62 MAX+ IR thermometer was manually pointed at several components (toroids, PAs, fuses, DC bus bar and current transformer) to cross-check the IR camera's accuracy. An Optris model CS LT pyrometer monitored the step-up network inductor, which is connected to the tube-in-tube cooling circuit of the PPU center conductor. The RF current going to the dummy load was measured using a Pearson current transformer connected to an oscilloscope. DC current was measured by a LEM current transducer model DHR-C420-500 fed to a Fluke multimeter.

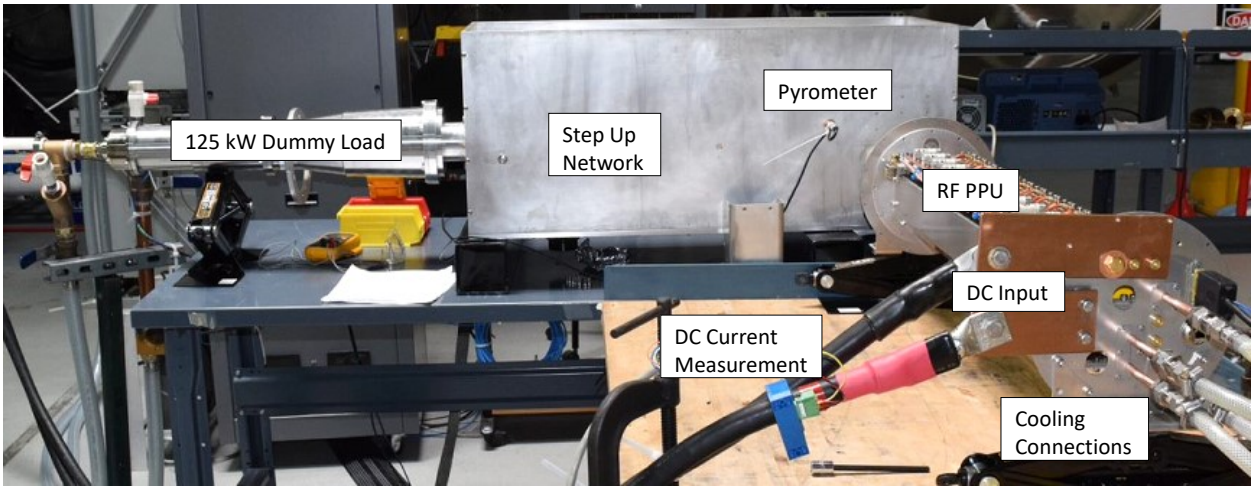

Fig. 11 Setting up for the full-power bench test at Ad Astra. The Step-Up Network box is over-sized for experimental convenience.

2. Full Power Bench Test Results

The complete RF PPU was brought to full power for the first-time on August 12, 2019 and completed steady-state operation for over an hour. Three rounds of tests brought the unit to 120 kW at varying DC voltages. The IR photos show a satisfactorily uniform distribution of heating for the parts. All surfaces indicated temperatures within operational limits. There was a modest variation in the combiner toroid temperatures, likely due to minor manufacturing differences. The DC fuses were the hottest components measured; they are designed to run hot so that they can react quickly to protect the solid-state devices downstream.

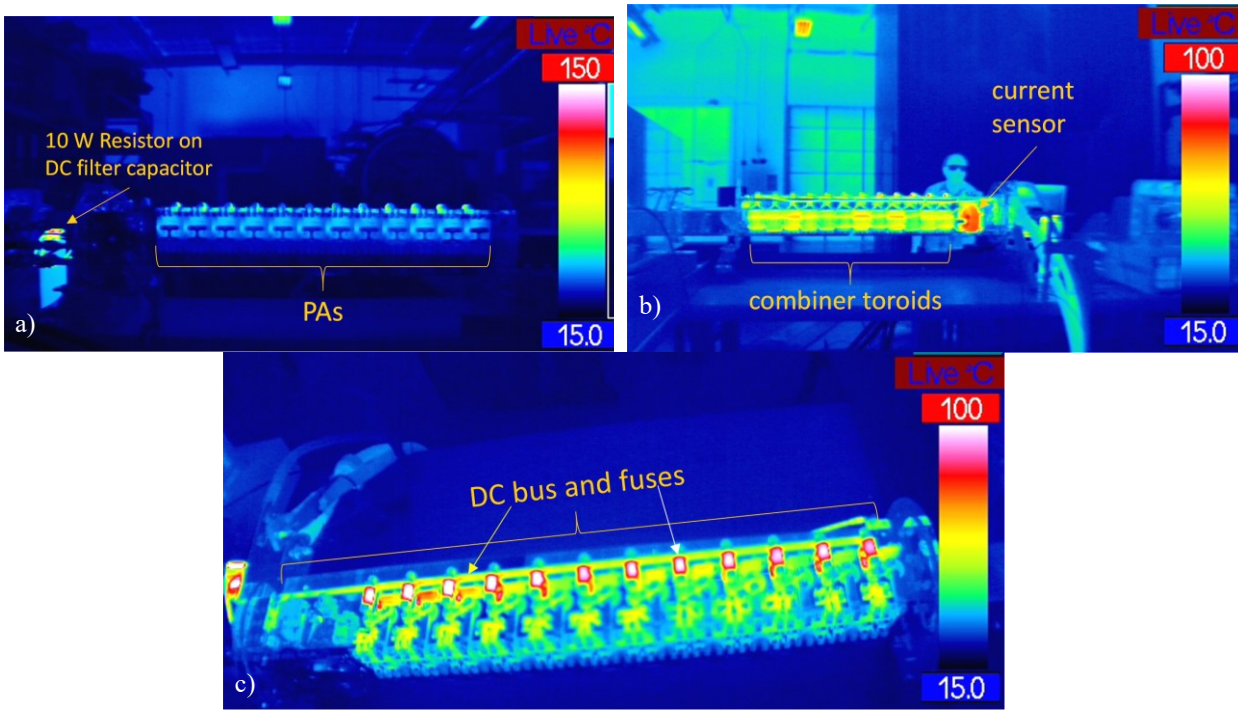

Fig. 12 Infrared images during the full power bench test at Ad Astra, showing a) the power amplifiers, b) the combiner toroids, and c) the DC bus and fuses.

D. Preparation for Vacuum Operation

After successful completion of the full-power bench tests, the PPU and step-up network were integrated into Ad Astra's main vacuum chamber. The mounting arrangement is shown in Fig. 8 and Fig. 14. An existing coaxial RF feedthrough was used to transmit RF power out of the chamber and to the same dummy load used in the full-power bench test. The dummy load was relocated to a more permanent mounting location, but the plumbing arrangement was functionally the same. As simplified water flow schematic is shown in Fig. 13.

Using an Agilent network analyzer, the step-up network variable capacitor was adjusted to present the correct impedance at the PPU output. Because this capacitor cannot be adjusted remotely, it was locked into position in preparation for the vacuum test.

Two new vacuum feedthroughs were installed for the DC power input to the PPU. To reduce bending stress at the metal-to-ceramic seals of the DC feedthroughs, the heavy cables (500 MCM) were strain-relieved at multiple locations on the air side of the chamber wall. Strain relieving on the vacuum side would have been more complicated, so the magnetic force on the DC conductors was analyzed to determine if support was necessary. The force due to the background field of the VX-200SS™ and the opposing DC currents was determined to be a small fraction of the feedthrough's weight, so the relatively short vacuum side conductors were left to cantilever.

The PPU and ISUN cooling connections were leak-checked using pressurized helium and a mass-spectrometer leak detector with a sniffer probe. The PPU coolant circuit was integrated into the existing VX-200SS™ cooling water circulation system, but with a dedicated pair of fluid feedthroughs at the chamber wall.

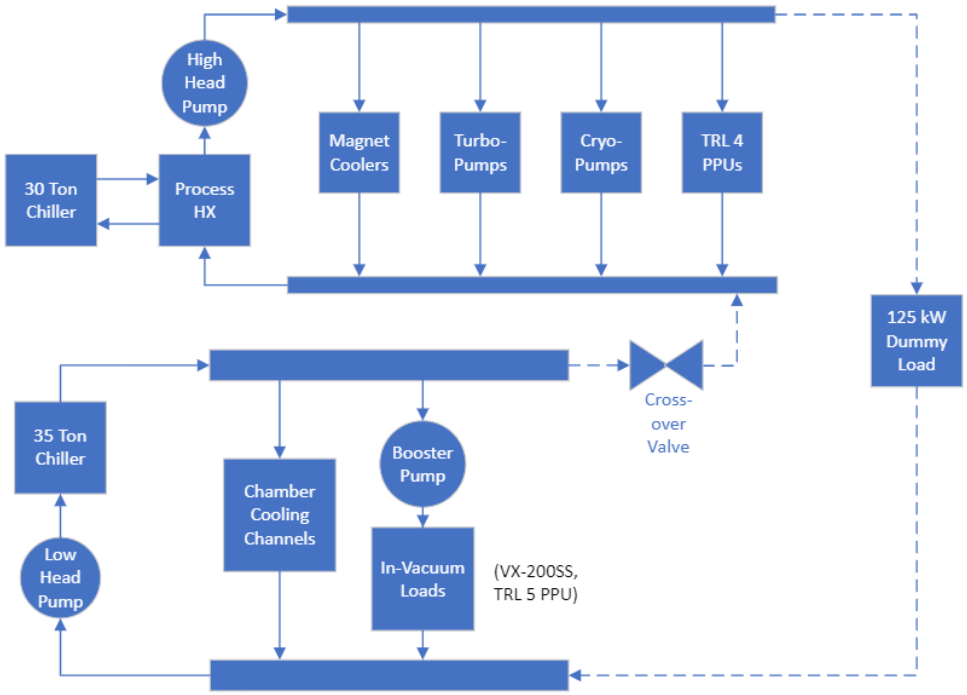

Fig. 13 Laboratory water systems reconfigured for 125 kW dummy load operation, dashed lines showing the additional plumbing. To support steady state cooling of the dummy load, the 30-ton chiller/HX and 35-ton chiller systems were partially serialized through the dummy load and a cross-over connection.

1. Vacuum Test Measurements

A LEM Voltage Transducer DVL-500 was installed upstream of the input DC power feedthrough. The LEM current transducer used during the bench test was also relocated upstream of the feedthrough. The DC sensors were connected to analog input channels in the external data acquisition system; these signals would be used as an independent measurement of input power to the PPU. Omega series PR-21 resistance temperature detectors (RTDs) were installed in the PPU coolant inlet and outlet connections inside the vacuum chamber. The signals from these were routed to the in-vacuum data acquisition system. To measure the PPU coolant flow, a Proteus model 06004BN2 paddle flow sensor was installed in the dedicated PPU branch cold leg just upstream of its chamber feedthrough. The pulse output from this sensor was connected to a digital input channel in the external data acquisition system. The RTDs at the PPU and the flow meter at the chamber feedthrough would be used to measure the heat loss produced by the PPU during operation.

The Pearson current transducer in the step-up network was again used to measure the RF output current from the PPU. The Pearson signal was fed out of the chamber with a coaxial feedthrough and recorded manually at an oscilloscope. Prior to the vacuum test, a network analyzer was used to measure the signal loss in the series of coaxial cables and connectors between the Pearson and the oscilloscope. This cable loss was subsequently used to correct the raw Pearson output.

2. PPU Control

The external PPU inhibit lines and dummy load water flow/temperature interlocks were integrated into the VX-200SS™ in-vacuum control system for long-term functionality. These interlocks are designed to minimize the risk of accidentally operating the dummy load without sufficient cooling.

For the initial vacuum test, the PPU was controlled by a PC-based graphic user interface that was developed by Aethera for its own testing. On January 15th, 2020, the PPU was operated at full power in the vacuum chamber with the main door open. This testing verified the functionality of the supporting systems and indicated that the laboratory was ready for operation of the PPU in vacuum.

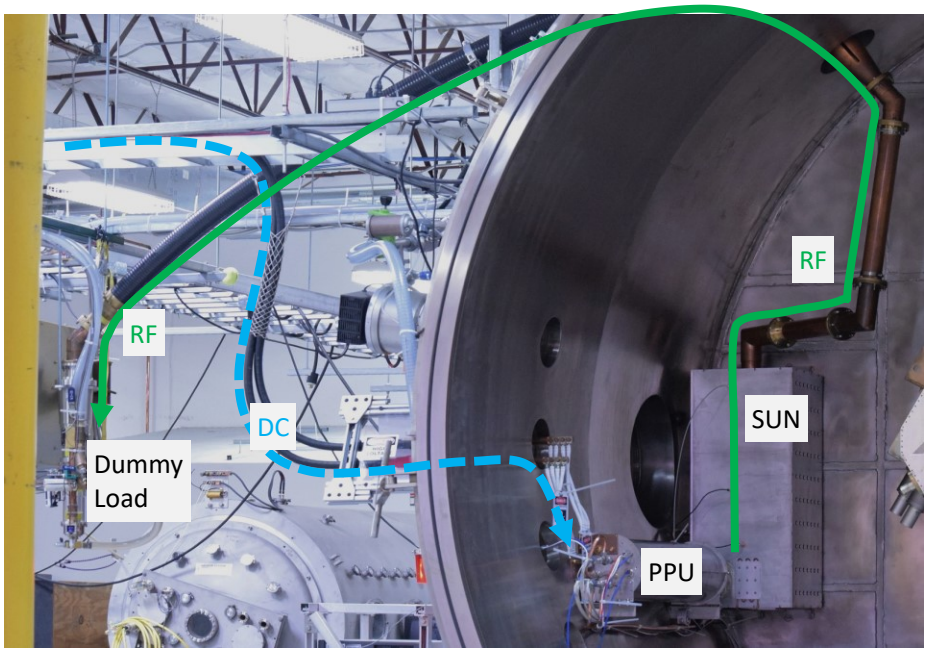

Fig. 14 Power flow and feedthrough arrangement during in-chamber PPU testing with the dummy load. The PPU and step-up network (SUN) are shown in their permanent locations. The rigid coaxial line can be reconfigured to connect the PPU to the VX-200SS™ plasma circuit.

3. Monitoring for Outgassing

The PPU materials of construction were expected to outgas when heated in vacuum for the first time, but there are no high-vacuum pressure sensors inside the PPU enclosure. To gauge the risk of an unwanted glow discharge forming internal to the PPU shield, Ad Astra compared the vacuum conductance of the enclosure (C_{PPU}) with that of the turbomolecular pumps (C_{turbos}). A simple model of the relationship between the pressure inside the PPU and that of the chamber was used to assess the risk.

$$P_{PPU} = P + \frac{C_{turbos}}{C_{PPU}}(P - P_{base}) \tag{1}$$

In equation (1), 'P' is the chamber pressure, 'P_{PPU}' is the pressure internal to the PPU enclosure, and 'P_{base}' is the chamber pressure prior to the PPU heating up. This model assumes that the PPU and the chamber are at the same pressure prior to RF operation. The conductance ratio 'C_{turbos}/C_{PPU}' is approximately 7.

After consulting Paschen limits for water vapor [10], it was determined that the existing chamber pressure sensors would provide sufficient warning the operator before the PPU's internal vacuum pressure reached a glow discharge threshold. To make it easier to detect a potentially dangerous outgassing rate, the vacuum test was planned with only the turbomolecular pumps operating (cryopumps off). A residual gas analyzer was also operated to monitor for unusual gas loads.

E. Vacuum Testing at Full Power

The main vacuum chamber was pumped down on January 16th, 2020, while hot water circulated through the PPU and step-up network to help drive out volatiles and condition the hardware to reduce the risk of a glow discharge. As discussed earlier, pumping was limited to the two turbomolecular pumps on the upstream section of the chamber.

The PPU vacuum operational test began on January 20th, 2020. Chamber pressure had reached the low 10^{-5} Torr scale and the PPU water was switched from hot to cold. DC bus voltage was set to 300 V. The PPU was operated in a series of 10 kW power steps, each interval averaging approximately 15 minutes in length. At each power step, the operators verified that the PPU temperatures and chamber pressure were within safe bounds and not rising too quickly. The PPU was operated at the full power setting of 120kW for nearly four hours. During the final 40 minutes of operation, the VX-200SS™ magnet was energized to full operational field strength.

During the vacuum test, the PPU telemetry was archived via the Aethera interface. The PPU water flow and water temperatures were archived from the Ad Astra LabVIEW interface. The DC input voltage and input current sensors were also archived from the LabVIEW interface. The PPU RF output current was measured by an oscilloscope. RF power was then calculated using Ohm's Law and the characteristic impedance of the transmission line and dummy load (50 Ω).

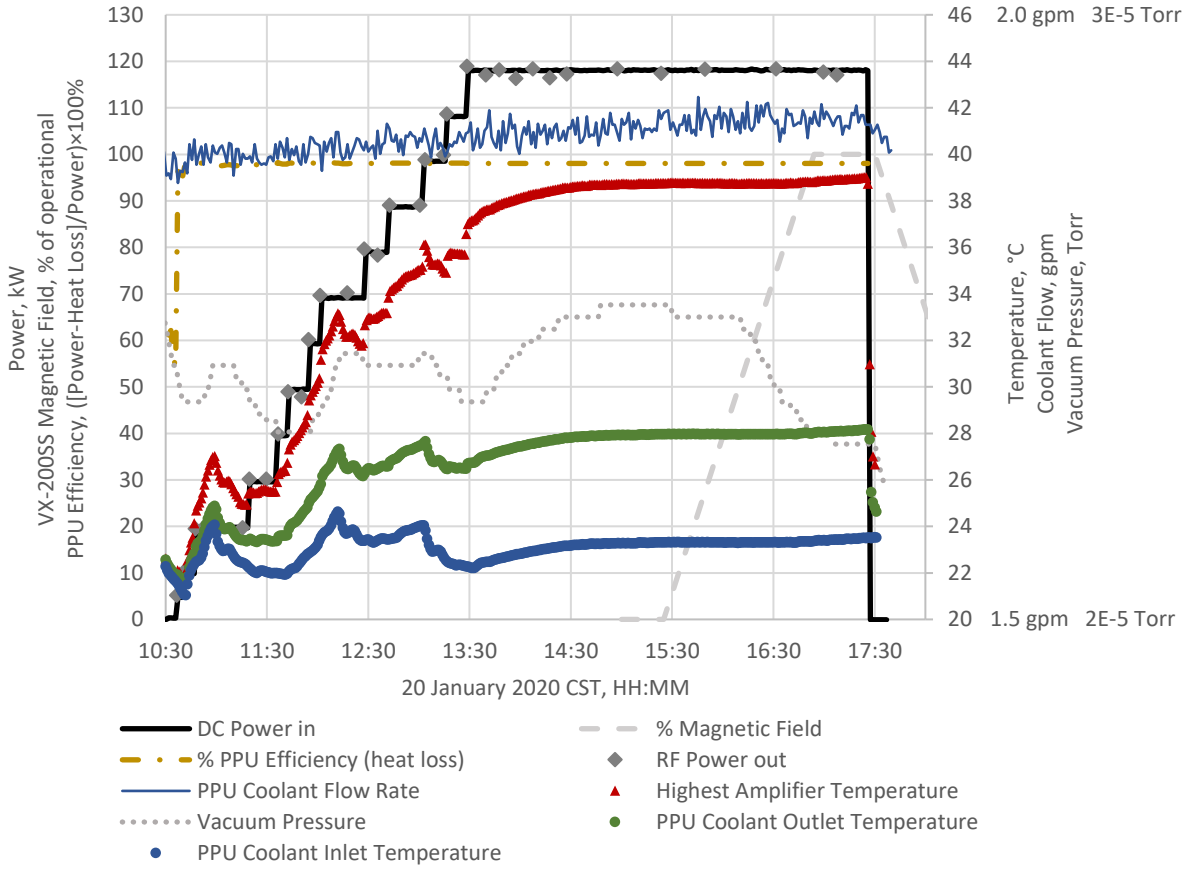

Fig. 15 PPU data versus time during the full-power vacuum test with magnetic field ramp. Variations in coolant inlet temperature are due to the thermostatic cycling of the chilled water system.

1. Vacuum Test Results

The vacuum test showed that the PPU was able to continuously resonate the dummy load at full power, in high vacuum, and in the stray field of the VX-200SS™ magnet. All temperatures were well within their operating limits, and the PPU was in thermal steady-state within the thermostatic variation of the chilled water temperature. During the final three hours of the full power run, the difference between the chilled water temperature and the highest power amplifier temperature increased by less than 0.1 °C; most of this increase was probably due to a slight effect of the VX-200SS™ magnetic field. The cooling water flow rate was not intentionally adjusted during the test; it varied by less than 0.1 gallons per minute during the full power run.

The chamber pressure showed little reaction to PPU operation, increasing from 2.3×10^{-5} Torr to 2.5×10^{-5} Torr at the beginning of the full power operation. The residual gas analyzer indicated that this pressure rise was mostly due to water vapor.

2. Full-Power Efficiency

The vacuum test allowed for another estimate of the PPU efficiency by measuring the heat lost to the PPU cooling water. In the installed configuration, there is some additional heat loss from the step-up network (SUN) inductor, as its water is in series with that of the PPU combiner. The losses therefore include those from the PPU cold plate, the PPU combiner conductor, and the SUN inductor, which are all in series from the flow meter at the chamber feedthrough. The RTDs measuring the PPU cooling water temperature are 1/8-inch diameter probes immersed in the water stream immediately outside the PPU enclosure. The efficiency calculation is summarized in Table 8 below. 'V_{DC}' and 'I_{DC}' are the input DC voltage and current, respectively. The water mass flow rate is '$\dot{m}$,' while 'c_p' is the specific heat of water. (T_{out}-T_{in}) is the difference between the PPU cooling water outlet and inlet temperatures.

Table 8 PPU efficiency determination by coolant heat loss based on average measurements during the vacuum test while at full background magnetic field strength.

DC input power: $P_{DC} = (V_{DC})(I_{DC})$	118.1 kW
PPU coolant heat: $P_{loss} = (\dot{m})(c_p)(T_{out}-T_{in})$	2.3 kW
PPU efficiency = $[1-(P_{loss}/P_{DC})]\times100\%$	98%

F. Operation with VX-200SS™

1. Connecting the PPU to the Rocket Core

After successful completion of the full-power vacuum test, the SUN was disconnected from the dummy load feedthrough and connected to the ICH Matching Network (MaN) via rigid coax. This allowed the PPU to resonate the VX-200SS™ rocket core during subsequent experimental campaigns, establishing the circuit shown in Fig. 3.

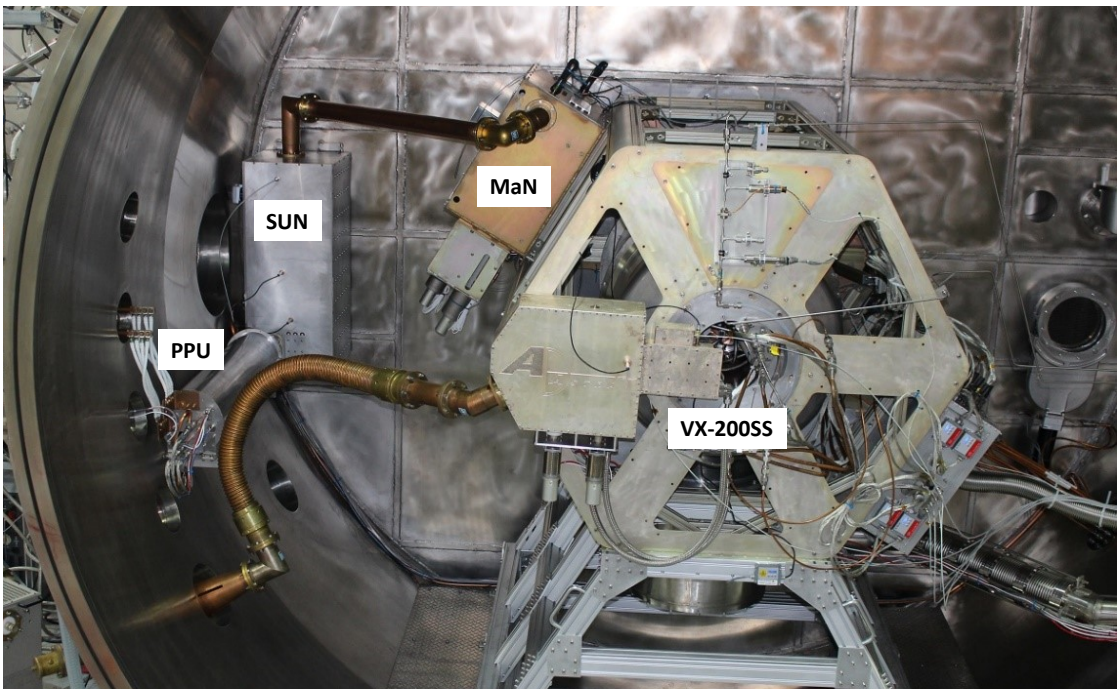

Fig. 16 The TRL-5 ICH PPU in its permanent configuration as part of the VX-200SS™ system. The coaxial lines have been reconfigured to connect the step-up network (SUN) to the matching network (MaN), which then connects to the rocket core.

2. Vacuum Resonating

Ad Astra and Aethera have jointly developed an operational technique by which the PPU can vacuum resonate the ICH coupler: an operation which involves driving a few kW of RF power into the rocket core with zero propellant flow. Vacuum resonating allows the coupler circuit to be energized at full RF voltage and current, but at a small

fraction of the operational power. This process can help identify limits in the voltage and current handling capability of the circuit. It also helps condition the system in preparation for plasma operations. Crucially, the new PPU can be tuned to the vacuum circuit using only the remotely adjustable capacitance in the MaN; it is not necessary to adjust the *fixed* capacitance in the SUN or the MaN. This ability allows Ad Astra to vacuum resonate the circuit and then proceed immediately to plasma operations, without having to vent the main chamber as an intermediate step.

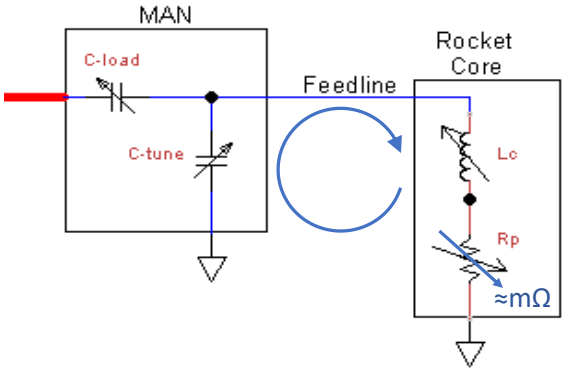

Fig. 17 VASIMR® circuit during vacuum resonating. With no propellant flow, the resistance Rp is reduced by several orders of magnitude, leaving only the resistance of the coupler material. RF current is recirculated between the matching network and the RF coupler to test the circuit's voltage and current handling and to prepare the conducting surfaces for plasma operation.

3. Control System Integration

The VX-200SS™ control system was modified to allow simultaneous control of the propellant flow, helicon power and ICH power, the latter via the TRL-5 PPU. The LabVIEW-based control system of the VX-200SS™ now incorporates communication with the Modbus interface of the PPU, which was briefly described in section II.B.4.

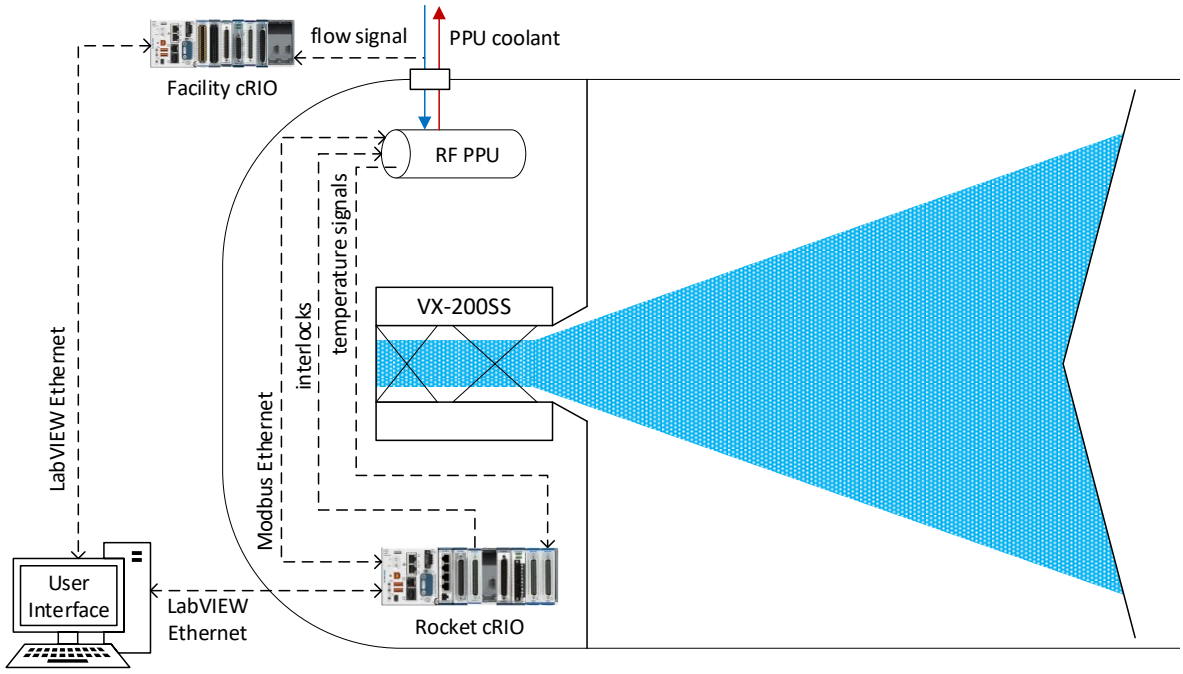

Fig. 18 Simplified schematic of the TRL-5 PPU integrated into the VX-200SS™ control system.

4. Plasma Operation

The robust impedance range of the TRL-5 ICH PPU allows the VX-200SS™ operator to pre-tune the matching network for high power operation. This simplifies operations because there is less of a requirement to dynamically tune the circuit during the power ramp; the PPU simply tolerates a moderately high VSWR at startup.

On July 30, 2020, the TRL-5 PPU drove the ICH circuit at nearly 70 kW for 18 minutes while the VX-200SS™ helicon stage simultaneously operated at nearly 30 kW, resulting in a total power of approximately 100 kW. This test allowed Ad Astra for the first time to reach and measure a steady-state temperature on the ICH section of the rocket core ceramics during 100 kW operation. The data from this campaign has enabled the continued development of the VX-200SS™ rocket core and has demonstrated progress toward the goal of steady state 100 kW operation.

IV. Conclusions and Outlook

A TRL-5 RF PPU for the ICH stage of the VASIMR® VX-200SS™ engine has been developed, manufactured, and tested, in thermal steady-state and a relevant environment, at approximately 120 kW of input power. The new PPU features state-of-the-art gallium nitride power transistors, presumably making it easier to transition the overall design to that of a spaceflight ready system. The PPU has demonstrated 98% efficiency with a power-specific mass of less than < 0.5 kg/kW.

A. Helicon PPU

The TRL-5 PPU needed for the VX-200SS™ helicon stage will use a design similar to that of the ICH PPU; the accomplishments described in this paper have retired most of the development risk. The remaining development items are low risk modifications associated with increasing the frequency by roughly an order of magnitude. The helicon PPU will be rated for approximately 50 kW of RF power and will therefore be a smaller unit. The higher frequency is estimated to increase the power conversion losses only slightly. The efficiency is expected to be better than 95% and the specific mass less than 1 kg/kW.

Fig. 19 APG7-50 commercial RF generator developed by Aethera Technologies. Modifying this design to produce an efficient, TRL-5 helicon PPU is expected to be straightforward.

1. Commercial APG7-50 Generator

Aethera has utilized the successful design of the TRL-5 ICH PPU to develop a 7 MHz product for commercial terrestrial applications: the APG7-50 generator. This generator is designed to fit in a standard 19-inch instrumentation rack and is only 4U high. The unit produces 50 kW of output power at 6.78 MHz and is frequency agile. The APG7-50 is 95% efficient from wall AC to RF power and is primarily conduction cooled.

By developing this commercial product, Aethera has already addressed the most significant challenges to producing a TRL-5 helicon PPU. The generator control system has demonstrated the impedance tolerance necessary for commercial loads, a quality which is also important for reliable plasma startup in VASIMR® system. The amplifier design and power control techniques are also demonstrated in this commercial product. Adaptation of the APG7-50 to a TRL-5 helicon PPU should therefore hold very low risk. The complete RF subsystem of the VX-200SS™ would then operate within a vacuum and magnetic environment that is relevant to a spaceflight VASIMR® engine.

B. Ad Astra and Aethera

The design, development, and testing process described in this paper has succeeded in all respects and has been satisfactory to both companies. The authors look forward to a continued partnership in future projects.

Acknowledgments

Development of the TRL-5 PPU was supported by private funds from the Astra Rocket Company with additional funding from the Canadian Space Agency (CSA) Space Technology Development Program (STDP). Development of the VASIMR® VX-200SS™ has been supported in part by Ad Astra private funds and by NASA's Next Space Technologies for Exploration Partnerships (NextSTEP).

References

[1] Chang Díaz, F. R., Squire, J. P., Carter, M. D., Corrigan, A. M. H., Dean, L., Farrias, J., Giambusso, M., McCaskill. G., and Yao, T. "An Overview of the VASIMR® Engine," *AIAA Propulsion and Energy Forum*, AIAA 2018-4416, AIAA, Cincinnati, OH, 2018.
doi: 10.2514/6.2018-4416

[2] Longmier, B. W., Squire, J. P., Olsen, C. S., Cassady, L. D., Ballenger, M. G., Carter, M. D., Ilin, A. V., Glover, T. W., McCaskill, G. E., Chang Díaz, F. R. and Bering III, E. A., "Improved Efficiency and Throttling Range of the VX-200 Magnetoplasma Thruster," *Journal of Propulsion and Power,* Vol. 30, No. 1, 2014, pp. 123-132.
doi: 10.2514/1.B34801

[3] Bourguignon, E., and Fraselle, S., "Power Processing Unit Activities at Thales Alenia Space in Belgium," *The 36th International Electric Propulsion Conference*, IEPC-2019-584, ERPS, Vienna, Austria, 2019.

[4] Soendker, E., Hablitze, S., Haynie, C., Hesterman, B., Poehls, A., Bachand, K., Dinca, D., Boomer, K., Pinero, L., and Birchenough, A., "13kW Advanced Electric Propulsion System Power Processing Unit Development," *The 36th International Electric Propulsion Conference*, IEPC-2019-692, ERPS, Vienna, Austria, 2019.

[5] Pearton, S. J., Ren, F., Patrick, E., Law, M. E., and Polyakov, A. Y., "Review-Ionizing Radiation Damage Effects on GaN Devices," *ECS Journal of Solid State Science and Technology*, Vol. 5, No. 2, 2015.
doi: 10.1149/2.0251602jss

[6] Muraro, J. L., Nicolas, G., Nhut, M. D., Forestier, S., Rochette, S., Vendier, O., Langrez, D., Cazaux, J. L., and Feudale, M., "GaN for space application: Almost ready for flight," *International Journal of Microwave and Wireless Technologies*, Vol. 2, No. 1, 2010, pp. 121-133.
doi: 10.1017/S1759078710000206

[7] Wellekens, D., Stoffels, S., Luu, A., Haussy, M., Mélotte, M., Agten, D., and Decoutere, S., "Architecture Choice for Radiation-Hard AlGaN/GaN HEMT Power Devices," *2017 17th European Conference on Radiation and Its Effects on Components and Systems (RADECS)*, IEEE, Geneva, Switzerland, 2017, pp. 1-5.
doi: 10.1109/RADECS.2017.8696192

[8] Notarianni, M., Messant, B., and Maynadier, P., "Using GaN HFET to replace MOSFET in DC/DC for space applications," *2019 European Space Power Conference (ESPC)*, IEEE, Juan-les-Pins, France, 2019, pp. 1-3.
doi: 10.1109/ESPC.2019.8931996

[9] Squire, J. P., Carter, M. D., Chang Díaz, F. R., Giambusso, M., Glover, T. W., Ilin, A. V., Oguilve-Araya, J., Olsen, C. S., Bering III, E. A., and Longmier, B. W., "VASIMR Spaceflight Engine System Mass Study and Scaling with Power," *The 33rdInternational Electric Propulsion Conference*, IEPC-2013-149, ERPS, Washington, DC, 2013.

[10] Škoro, N., Marić, D., Malović, G., Graham, W. G., and Petrović, ZL., "DC Breakdown in Water Vapour at Low Pressures," *The 20th European Sectional Conference on Atomic and Molecular Physics of Ionized Gases*, Novi Sad, Serbia, 2010.